Ecological Modelling 384 (2018) 154–167

Contents lists available at ScienceDirect

Ecological Modelling

journal homepage: www.elsevier.com/locate/ecolmodel

# Effects of climate and soil conditions on the productivity and defence capacity of *Picea abies* in Sweden—An ecosystem model assessment

Anna Maria Jönsson*, Fredrik Lagergren

*Department of Physical Geography and Ecosystem Science, Lund University, SE-223 62 Lund, Sweden*

ARTICLE INFO

*Keywords:*
Climate impact assessment
Ips typographus
LPJ-GUESS
Non-structural carbohydrates
RCP 8.5
Boreal coniferous forest

ABSTRACT

Climate change can lead to an increased frequency of extreme weather events, which may induce a decline in tree vitality, rendering the forest more vulnerable to other stress factors. In this study we used the ecosystem model LPJ-GUESS to compare the NPP of boreal conifers on till soil and sandy soil, simulating the growth of Norway spruce during the 21st century using climate model projections corresponding to RCP 8.5. Model runs with and without nitrogen cycling enabled, in combination with two different approaches to implement the dynamics of non-structural carbohydrates (NSC) were compared. The simulations showed that the forest productivity in Sweden is influenced by an interplay between site-specific temperature conditions and precipitation. Local differences in soil conditions can have an impact on the productivity, mediated by soil water and nutrient content. A warmer climate will lead to a longer growing season, but the productivity increase will partly be offset by a higher frequency of drought stress in summer and higher autotrophic respiration in winter. The ecosystem model runs indicated that periods with drought stress can cause low NSC levels, leading to time periods with decreased defence capacity against attacks by secondary agents such as bark beetles. The risks may however not become apparent until the forest stands are middle-aged. The model results are discussed in relation to current forestry practice, with Norway spruce (*Picea abies*) commonly being planted on dry soils better suited for Scots pine (*Pinus sylvestris*) in order to reduce moose browsing damage of seedlings, which in the longer term may create a forest landscape more sensitive to spruce bark beetle attacks.

## 1. Introduction

Climate change can lead to an increased frequency of extreme weather events (IPCC, 2013), which may induce a decline in tree vitality, rendering the forest more vulnerable to other stress factors (Breda et al., 2006). Experiences from the 2003 heat wave in Europe indicate that exceedance of species-specific physiological tolerance limits and subsequent attacks by forest pests may threaten entire forest stands (Archaux and Wolters, 2006; Desprez-Loustau et al., 2006; Rouault et al., 2006; Seidl et al., 2008). The boreal coniferous forest of northern Europe is to a large extent managed as even-aged monocultures, with final felling (clear cutting) followed by planting of seedlings. The 50 to 150 years rotation periods of even-aged forest stands indicate that future scenarios should be taken into account at the timing of regeneration, to enable sustained production levels and risk management (Jönsson et al., 2015).

Norway spruce (*Picea abies*) is the most common tree species in Swedish forests followed by Scots pine (*Pinus sylvestris*), accounting for 42% and 39% of the total standing volume, respectively (Christiansen, 2014). In recent years, many forest owners have regenerated Scots pine forest stands with Norway spruce, as spruce seedlings are less palatable than pine seedlings and thereby suffer less from heavy browsing by the moose (*Alces alces*) (Bergqvist et al., 2001; Bergström and Bergqvist, 1999). Tree growth and vitality are highly influenced by environmental conditions, and Norway spruce grows better on till soils than Scots pine, but is more sensitive to dry spells and root rot on sandy soils (Bergquist et al., 2005; Bergqvist, 2016). This have created a concern that spruce stands on pine soils may perform less well in the future, in particular after being exposed to a severe drought stress (Bergqvist, 2016). The concern includes that drought stress may predispose the spruce trees to attacks by the spruce bark beetle (*Ips typographus*), which is capable of killing millions of mature spruce trees during outbreaks (Marini et al., 2017).

The issue described above is strongly linked to the potential impact of climate change and the development of adaptation strategies. A warmer climate may be beneficial for the forestry sector in northern Europe, resulting in a longer growing period with increased productivity (Bergh et al., 2003; Eriksson et al., 2015; Koca et al., 2006).

* Corresponding author.
*E-mail address:* Anna_Maria.Jonsson@nateko.lu.se (A.M. Jönsson).

https://doi.org/10.1016/j.ecolmodel.2018.06.023
Received 26 September 2017; Received in revised form 19 June 2018; Accepted 21 June 2018
Available online 17 July 2018
0304-3800/ © 2018 Elsevier B.V. All rights reserved.

However, climate change may also increase the risk of storm damage, particularly in spruce forests, as a consequence of increased occurrence of unfrozen soil and heavy precipitation during autumn and winter months when wind storms are common (Jönsson et al., 2015). Spruce bark beetle outbreaks are commonly triggered by storm events, as stormfelled spruce trees with low defence capacity can lead to rapid population build-up, which triggers aggregated attacks on living trees (Jönsson et al., 2012). Heat spells and drought often aggravate bark beetle outbreaks (Christiansen and Bakke, 1988), as warm weather can trigger flight activity of bark beetles in late summer (Jönsson et al., 2011) and tree drought stress can lead to lowered defence capacity (Netherer et al., 2016).

Coniferous trees have constitutive as well as induced defence systems (Christiansen and Bakke, 1997). The constitutive defence consists of resin ducts and the activation of the induced defence, e.g. by bark beetle attacks, leads to mass production of resin and formation of reaction zones (Franceschi et al., 2005; Zhao et al., 2011). The tree defence capacity is linked to the amount of carbohydrates that can be used for defensive reactions (Christiansen et al., 1987; Guerard et al., 2007). The storage of non-structural carbohydrates (mainly mobile carbohydrates and starch) can be used as a proxy for assessing tree vulnerability and response to climate stress (Breda et al., 2006), as trees allocate energy resources to storage reserves in order to meet seasonal demands and buffer for stressful events (Chapin et al., 1990; Hoch et al., 2003). Climate change with warmer winters may have a negative impact on the storage, as the temperature dependent maintenance respiration will increase at a time when the light dependent photosynthesis is low or inactive (Kalberer et al., 2006).

Ecosystem modelling is useful for assessing potential future conditions, and model assessments of climate impact on primary production, risk of storm damage and subsequent bark beetle attacks have been carried out (Jönsson et al., 2015, 2012; Lagergren et al., 2012). However, ecosystem model assessments are commonly performed at a regional to global scale, and local differences in soil conditions or carry-over effects conveyed by non-structural carbohydrates are generally not accounted for. In this study we therefore applied the ecosystem model LPJ-GUESS to assess potential climate effects on tree vitality, quantified in terms of annual net primary production (NPP) and amount of non-structural carbohydrates (NSC) as proxies of bark beetle defence capacity. Model runs with and without nitrogen cycling enabled, in combination with two different approaches to quantify NSC were compared to assess the effect of model setup. To address climate change effects, we used an ensemble of climate model data corresponding to RCP 8.5, and focused on climate impacts on net primary production, autotrophic respiration during winter and soil water content, covering a range of climate factors and soil conditions. Our hypothesis was that an increase in NPP caused by a warmer climate will be offset both by dry spells during summer and elevated winter time respiration, with spruce stands planted on sandy soils being more prone to negative effects in terms of low NSC storage than spruce stands on till soils.

## 2. Material and methods

### 2.1. Dynamic vegetation model

The dynamic vegetation model LPJ-GUESS simulates the development of plant individuals through the processes of establishment, growth and mortality, and the simulated vegetation development takes generic natural disturbances into account (Smith et al., 2001). The model has mechanistic representation of the competition for resources, and it includes stocks and fluxes to simulate the ecosystem's water and carbon cycles (Smith et al., 2001). We used this model as it has been adapted to simulate the effect of formal management schemes representative of Swedish forest management practice, including planting of seedlings to generate an even-aged monoculture forest stand, pre-commercial thinning, thinning and clearcutting (Lagergren et al., 2012). LPJ-GUESS accounts for the $CO_2$ fertilization effect, also leading to an increased water use efficiency, and for the temperature effect on tree photosynthesis with a warmer climate leading to a longer growing season. LPJ-GUESS estimates of NPP are in line with other terrestrial carbon cycle models as well as data from FACE experiments (Piao et al., 2013). Furthermore, model code to capture the nitrogen cycle has recently been implemented, which influences the photosynthesis as well as the proportion of carbon allocated between above ground and below ground biomass (Smith et al., 2014). The vegetation dynamics is simulated for patches, representing an area of 1000 $m^2$, in which the plant individuals are grouped in age-class and species specific cohorts. The model requires a spin-up period of 400 years to allow for soil formation and establishment of forest vegetation. Plant functional types are distinguished by the parameter settings of climatic limits for establishment and survival, temperature response of phenology and photosynthesis, tree allometry, turnover rates, root distribution and drought tolerance. The model simulations of this study included two plant functional types: boreal coniferous forest parameterised for Norway spruce and an understory layer represented by C3 grass.

### 2.2. Climate data

LPJ-GUESS is driven by gridded climate data, using daily data on temperature, precipitation and radiation, and annual data on $CO_2$ concentration and nitrogen deposition. Data used in this study were selected from the EURO-CORDEX ensemble of regionally downscaled climate model scenario data for 1971–2099 with a daily temporal resolution and a spatial resolution of $0.44 \times 0.44^{\circ}$ (approximately $50 \times 50$ km) (Kotlarski et al., 2014). For the spin-up period, with the first simulation year corresponding to real-year 1500, the 1971–2000 period of climate data was repeated to generate a stable baseline.

To assess the effect of a distinct climate change signal, climate model data representing radiative concentration pathway (RCP) 8.5 (Moss et al., 2010) were used. The data were selected in a two-step procedure: In the first step, the temperature and precipitation data of all the 11 ensemble members representing RCP 8.5 had been bias corrected according to the quantile mapping method (Wilcke et al., 2013) using Mesan-EURO4M as reference. In the second step, a hierarchical cluster analysis was performed to extract a representative sub-ensemble (Wilcke and Bärring, 2016), with the aim of reducing the number of time-consuming ecosystem model simulations without losing information on potential climate development and uncertainties represented by the overall ensemble. The hierarchical cluster analysis was based on data from two time periods 1971–2000 and 2059–2098 and three measures of importance for vegetation growth: 1) cumulative degree days above 5 °C, 2) temperature and precipitation in spring and summer, May to July, and 3) temperature and precipitation in late summer and autumn, August to October. By this procedure, four representative ensemble members were identified (Table 1), corresponding to ***factor 7*** in the analysis of model results (details are provided in Section 2.4). $CO_2$ concentration associated with RCP8.5 was obtained from the RCP database (http://tntcat.iiasa.ac.at:8787/RcpDb).

### 2.3. Model settings

Model simulations combining ***seven factors*** with different parameter settings were performed to generate an ensemble of LPJ-GUESS model runs, to quantifying model trends over space and time as well as model uncertainties (Fig. 1). Two of the factors relate to site conditions; (***1***) three sites were selected to capture large-scale environmental gradients and (***2***) local variations in soil conditions were assessed for each site by including simulations representing two soil texture classes, sand and till. Two of the factors relate to temporal aspects of climate change and forest stand development; (***3***) three time periods (2010–2029, 2040–2059 and 2080–2099) were selected to capture the impact of

**Table 1**
The EURO-CORDEX ensemble contained eleven model simulations with different GCM-RCM combinations that all represent RCP 8.5 (Moss et al., 2010). A hierarchical cluster analysis was applied to obtain a representative sub-ensemble, in order to reduce the number of ecosystem model simulations needed, without losing information on the potential climate development and uncertainties represented by the overall ensemble (Wilcke and Bärring, 2016). The selected sub-ensemble contained four members (**in bold**).

| GCM | RCM |
|---|---|
| **CanESM2** | **SMHI-RCA4** |
| **CERFACS CNRM CM5** | **SMHI-RCA4** |
| EC-EARTH | DMI HIRHAM5 |
| **EC-EARTH** | **KNMI RACMO22E** |
| EC-EARTH | SMHI-RCA4 |
| GFDL-GFDL ESM2M | SMHI-RCA4 |
| HadGEM2-ES | SMHI-RCA4 |
| **IPSL CM5A MR** | **SMHI-RCA4** |
| M-MPI-ESM-LR | SMHI-RCA4 |
| MIROC5 | SMHI-RCA4 |
| NorESM1-M | SMHI-RCA4 |

climate change during the 21st century according to scenario RCP 8.5, and (***4***) three forest stand age classes, corresponding to young, mid-age and mature forest were simulated to assess differences over a rotation period. The three final factors address model uncertainties by (***5***) comparing LPJ-GUESS simulations with and without nitrogen cycling enabled, (***6***) using two different approaches to quantify NSC, and (***7***) comparing model runs driven by different climate model datasets.

Model simulations were carried out for three sites in Sweden (***factor 1***), situated in the counties of Kalmar, Värmland and Västernorrland (figure abbreviations: Värml. and V.norrl.). Each site corresponds to a climate grid cell, and the sites were selected to capture different environmental conditions (Table 2) according to the following three criteria: i) The sites should cover a distinct gradient in latitude, and consequently also in temperature and day length. ii) The sites should cover a gradient in the difference between potential and actual evapotranspiration. iii) The sites should be situated in a region with severe browsing of pine saplings, which have led to a high fraction of the drier sites most suitable for Scots pine being regenerated with Norway spruce. For site selection (Table 2), hydrological information was obtained from the Swedish Hydrological Meteorological Institute (www.smhi.se/klimatdata/hydrologi/avdunstning, 2017-05-15). Sapling damage and regeneration information was obtained from the Swedish moose browsing inventory in 2016 by the Swedish Forest Agency (https://skogsstyrelsen.se/abin, 2017-05-15).

**Table 2**
The three sites included in this study were selected based on a range of selection criteria, and the table display the corresponding information. Hydrological data was obtained from the SMHI (www.smhi.se/klimatdata/hydrologi/avdunstning, 2017-05-15), and data on regeneration on sapling damage caused by moose browsing from the Forest Agency (https://skogsstyrelsen.se/abin, 2017-05-15). Data of standing volume per hectare by different age classes (including all species and productivity classes, which is the highest reported level of detail) from the Swedish national forest inventory (Nilsson And Corey, 2013) was scaled to C biomass using biomass expansion factors for spruce and pine (Lehtonen et al., 2004) weighted with the standing volume of the two species respectively and a biomass C fraction of 50% (Sandström et al., 2007).

| County | Kalmar | Värmland | Västernorrland |
|---|---|---|---|
| Latitude | 57.0 °N | 60.0 °N | 63.2 °N |
| Potential - actual evapo-transpiration 1961–1990 (mm) | 200 | 100 | 150 |
| Annual precipitation 1961–1990 (mm) | 650 | 850 | 750 |
| Fraction of pine stems damaged by browsing | 76% | 54% | 46% |
| Fraction of pine stems damaged during the last year | 12% | 11% | 14% |
| Fraction of dry soils regenerated with spruce, not pine | 36% | 28% | 27% |
| Tree biomass for 0-19 year age-class (kg C $m^{-2}$) | 1.0 | 0.9 | 0.6 |
| Tree biomass for 30-49 year age-class (kg C $m^{-2}$) | 7.3 | 6.6 | 5.7 |
| Tree biomass for 80-99 year age-class (kg C $m^{-2}$) | 10.8 | 10.4 | 9.0 |

To assess the effect of soil conditions (***factor 2***) on tree vitality, the simulations were done for both moist soil and dry soil types, differing in the parameterisation of $K$ and $H_{max}$ (Table 3 in Haxeltine and Prentice, 1996). $K$ is the empirical scalar of the water-content dependent percolation from the upper soil layer to the lower soil layer (mm $day^{-1}$, the percolation at field capacity of the upper layer). $H_{max}$ is the fraction of available water (volume fraction of water at field capacity minus fraction of water at wilting point). The moist soil type represents a till with high fraction of silt and clay ($K$ = 4 mm $day^{-1}$, $H_{max}$ = 16%),

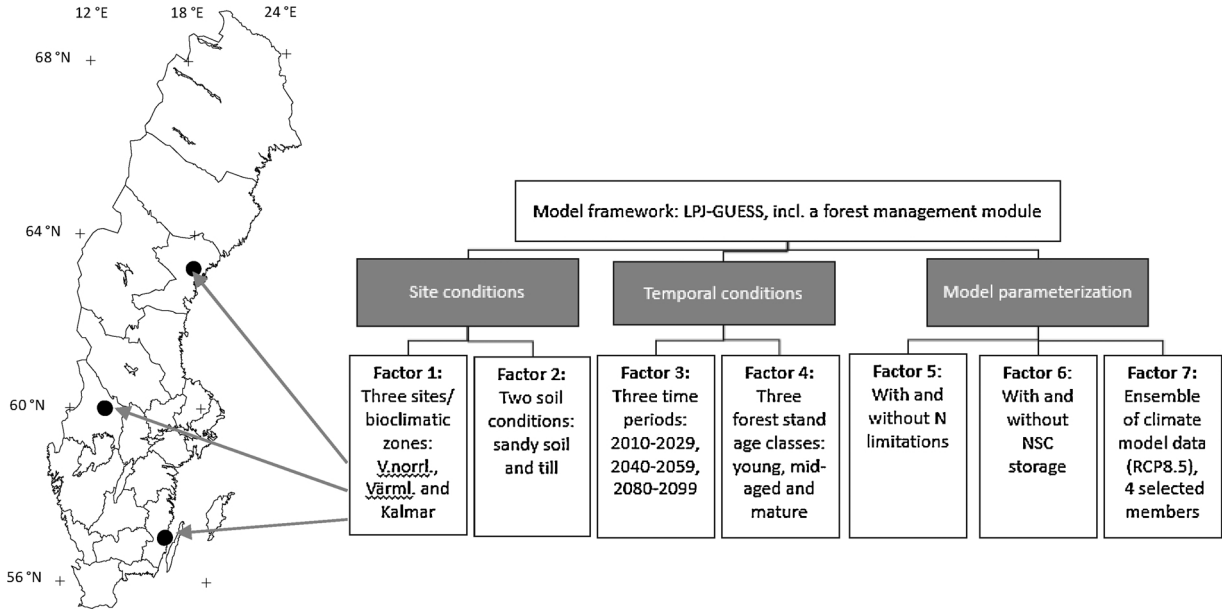
12 °E
18 °E
24 °E
68 °N
64 °N
60 °N
56 °N
Model framework: LPJ-GUESS, incl. a forest management module
Site conditions
Temporal conditions
Model parameterization
Factor 1: Three sites/ bioclimatic zones: V.norrl., Värml. and Kalmar
Factor 2: Two soil conditions: sandy soil and till
Factor 3: Three time periods: 2010-2029, 2040-2059, 2080-2099
Factor 4: Three forest stand age classes: young, mid-aged and mature
Factor 5: With and without N limitations
Factor 6: With and without NSC storage
Factor 7: Ensemble of climate model data (RCP8.5), 4 selected members

**Fig. 1.** a) Location of the three study sites. b) Conceptual diagram of the model study design.

**Table 3**
Analysis of variation among factors (county, period, soil type, age class, N limitation setting, NSC accounting and climate data) in relation to simulated annual NPP, non-structural C storage, winter NPP ($NPP_w$, Oct–Feb), normalized winter NPP ($NPP_{wn}$) and percent of years with a dry June, July and August. In this study, a monthly mean soil water content (SWC) in the upper soil layer < 0.2 was used as a proxy of drought. For each variable, the numeric values indicate the average value of all members within a factor, and the letters indicates significant differences within groups of factors.

| | Variable | | | | | | | |
|---|---|---|---|---|---|---|---|---|
| Factors | NPP $kg\,m^{-2}$ | NSC $kg\,m^{-2}$ | Biomass $kg\,m^{-2}$ | $NPP_w$ $g\,m^{-2}$ | $NPP_{wn}$ $g\,kg^{-1}$ | $June_{dry}$ % of years | $July_{dry}$ % of years | $August_{dry}$ % of years |
| V.norrl | 0.290 a | 0.327 a | 2.38 a | −20.5 c | −12.5 a | 11.3 a | 10.2 a | 2.5 a |
| Värml. | 0.333 c | 0.386 b | 2.80 c | −27.5 a | −12.6 a | 11.2 a | 13.1 b | 5.2 b |
| Kalmar | 0.319 b | 0.382 b | 2.65 b | −25.9 b | −12.0 b | 14.9 b | 16.9 c | 11.3 c |
| 2010–2029 | 0.290 a | 0.335 a | 2.36 a | −16.9 c | −10.0 c | 9.6 a | 13.8 b | 3.5 a |
| 2040–2059 | 0.320 b | 0.373 b | 2.65 b | −22.7 b | −11.4 b | 13.8 b | 11.8 a | 7.0 b |
| 2080–2099 | 0.332 c | 0.386 c | 2.83 c | −34.2 a | −15.7 a | 14.1 b | 14.7 b | 8.5 c |
| Till | 0.352 b | 0.415 b | 3.01 b | −29.4 a | −13.1 a | 5.8 a | 11.1 a | 5.8 a |
| Sand | 0.276 a | 0.314 a | 2.22 a | −19.8 b | −11.6 b | 19.2 b | 15.7 b | 6.9 b |
| Age 0–19 | 0.221 a | 0.160 a | 0.57 a | −11.0 c | −19.0 a | 8.6 a | 9.2 a | 4.3 a |
| Age 30–49 | 0.383 c | 0.507 c | 2.64 b | −30.5 b | −11.2 b | 15.1 c | 15.9 b | 7.6 b |
| Age 80–99 | 0.338 b | 0.427 b | 4.62 c | −32.4 a | −6.9 c | 13.8 b | 15.1 b | 7.1 b |
| N lim off | 0.306 a | 0.366 ns | 2.72 b | −18.7 b | −9.2 b | 17.3 b | 17.6 b | 8.2 b |
| N lim on | 0.322 b | 0.364 ns | 2.51 a | −30.6 a | −15.5 a | 7.7 a | 9.2 a | 4.5 a |
| NSC off | 0.334 b | – | 2.80 b | −28.2 a | −12.7 a | 13.1 b | 14.2 b | 6.7 b |
| NSC on | 0.294 a | – | 2.42 a | −21.0 b | −12.1 b | 11.9 a | 12.6 a | 5.9 a |
| Canesm | 0.317 b | 0.372 b | 2.65 b | −25.7 b | −12.8 a | 11.6 c | 10.3 b | 9.8 b |
| Cerfacs | 0.354 d | 0.407 d | 2.97 d | −27.1 a | −11.6 b | 5.8 a | 9.1 b | 2.8 a |
| EC-earth | 0.258 a | 0.290 a | 2.03 a | −19.5 c | −13.1 a | 23.5 d | 26.8 c | 9.5 b |
| IPSL | 0.327 c | 0.389 c | 2.79 c | −26.3 ab | −12.1 b | 9.1 b | 7.4 a | 3.2 a |

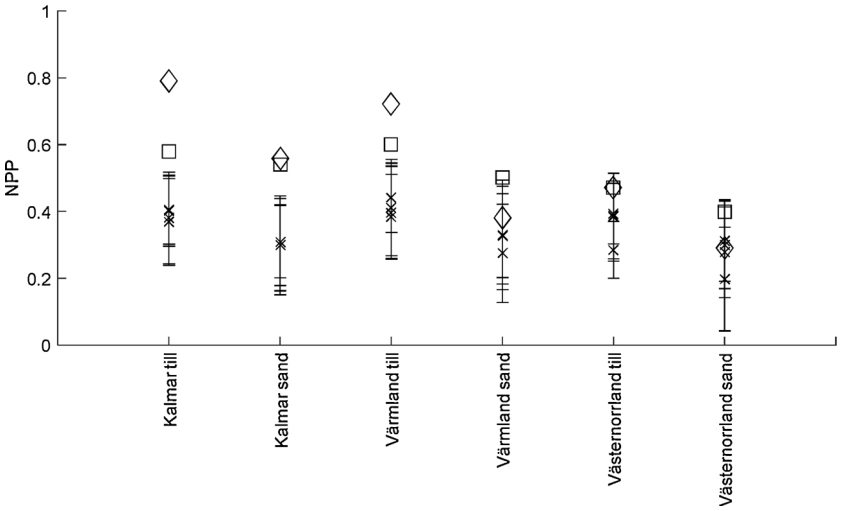


**Fig. 2.** Comparison between modelled NPP for boreal coniferous forest and NFI based county level estimates (Nilsson and Corey, 2013) for sandy soil and till soil at the three study sites. Average model estimates are indicated by **x** and the whiskers display the 95% confidence interval for the ensemble of model runs (Table 1), □ indicate the observed county levels for Scots pine, and ◊ the observed county levels for Norway spruce.

whereas the dry soil type represents a coarse, well sorted sandy soil ($K$ = 5 mm $day^{-1}$, $H_{max}$ = 4%). In both soils the upper soil layer was 0.5 m deep and the lower 1.0 m, which implies that the maximum store of available water was 240 mm (80 mm in upper layer) in the till, and 60 mm (20 mm in upper layer) in the sand. The parameters for the root distribution in Norway spruce were set to 80% of the roots in the upper layer and 20% in the lower layer (Rosengren and Stjernquist, 2004).

For each period, three age classes were simulated; a young (0–19 years), a mid-age (30–49 years) and an old forest stand (80–99 years) (***factor 4***). Ten patches were simulated for each age class, providing replicates that differ in the history of random disturbance events during the spin-up period. Forest management started in 1780–1860 (depending on what age class and period to be simulated) by turning natural disturbance off and implementing 100-years rotation periods with harvesting of tree stem biomass. For example, the patches with trees that were 30–49 years old in 2040–2059 had been clear-cut three times, in 1810, 1910 and 2010. After harvest, natural regeneration of conifers was simulated to occur, to generate even-aged monocultures. To account for site specific differences in productivity and resulting timing of management, pre-commercial thinning (PCT) was implemented at a stand age of 8, 9 and 11 years in Kalmar, Värmland and Västernorrland, respectively, allowing a maximum of 2300, 2000, and 1680 saplings per ha. The PCT was done from below, by taking away the youngest cohorts in first order. After the PCT, no further tree establishment was allowed. Natural disturbances were not simulated for managed forests, in order to generate results that were not influenced by confounding, random factors.

Model runs were carried out both with and without N cycling (***factor 5***), using gridded historical and RCP 8.5 scenario data of N deposition (Lamarque et al., 2010, 2011). That is, with N cycling enabled the nitrogen cycle is explicitly modelled, including deposition, biological N fixation, uptake by vegetation, losses by leaching, and decomposition of soil organic matter as influenced by the C:N ratio, soil water content, temperature and texture (Smith et al., 2014). An

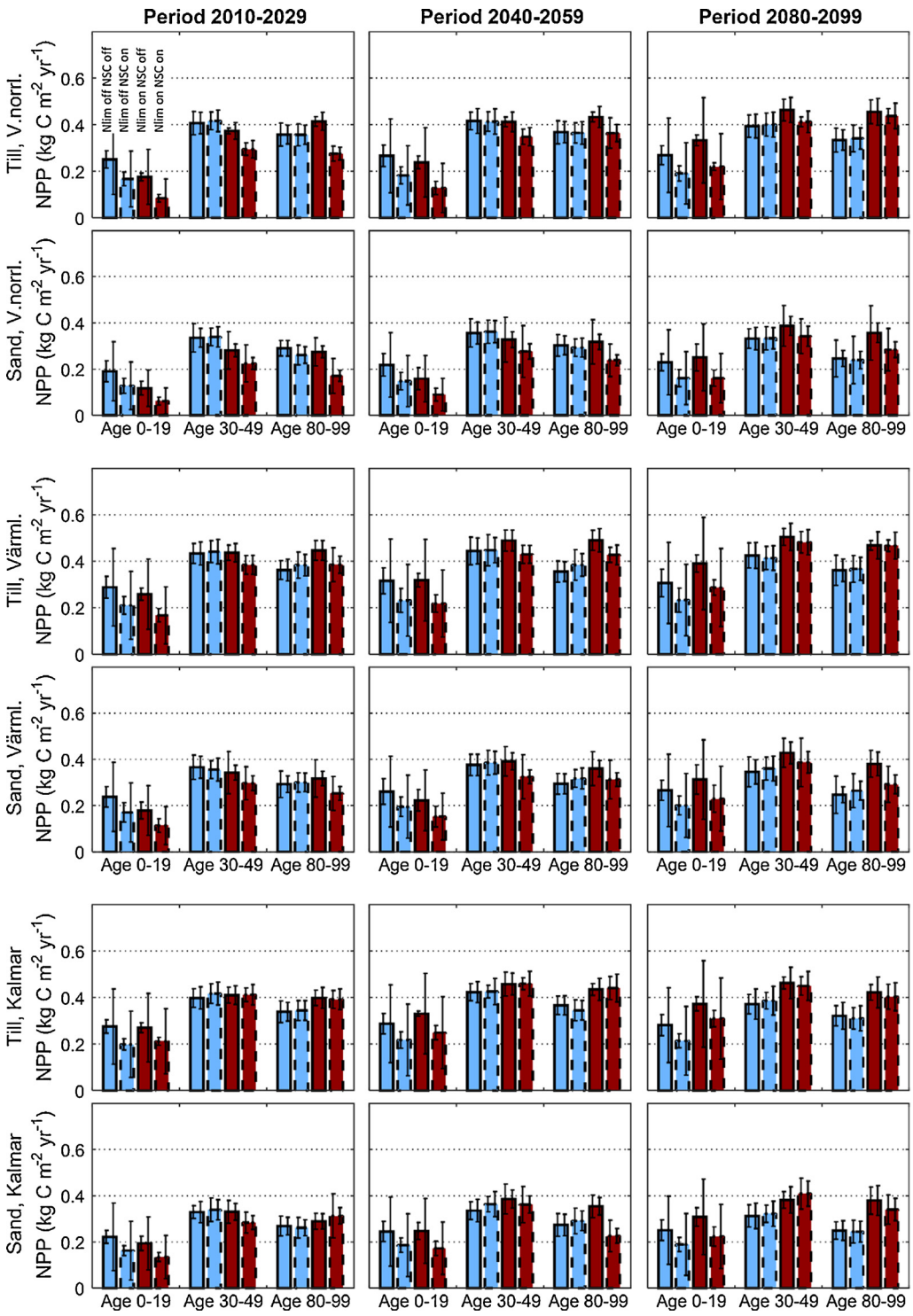


**Fig. 3.** Average annual NPP over 20 year periods and the 4 climate data sets for different periods, age-classes, soil types and counties. The four bars within each age-class represent the combinations of N cycling off (blue bars) or on (red bars), and NSC accounting off (solid contour line) or on (dashed line). The left error-bars show the variation of the mean ( ± one standard deviation) among model runs with four different climate model datasets, and the right error-bars show the inter-annual variation ( ± one standard deviation, mean of four model runs). (For interpretation of the references to colour in this figure legend, blue appears as grey and red as black in black and white print.)

important difference between the two model runs was the parameterisation of $\alpha_a$ that reduce quantum efficiency ($CO_2$ assimilation per unit photosynthetic active radiation absorbed) from leaf to canopy level; $\alpha_a$ was set to 0.55 without N cycling and 0.70 with N cycling enabled, with the photosynthetic efficiency being dynamically reduced by N limitations. Furthermore, the autotrophic respiration is linked to the C/N in living biomass, which is flexible with N cycling and fixed without. The $\alpha_a$ values have been calibrated by Smith et al. (2014) to obtain comparable global-scale estimates of the main ecosystem C stocks and flows with both settings for the period 1961–1990.

This study includes two different approaches to quantify NSC (***factor 6***). The model runs with the two different settings were denoted "NSC off" and "NSC on", respectively, differing in how the NSC is linked to a loan or a storage, and scaled in relation to the carbon mass in sapwood or canopy. The original LPJ-GUESS code (NSC off) does not explicitly account for NSC storage, but during years when the biomass increment in terms of allocation of resources to leaves and fine roots exceeds available resources, a loan of up to 80% of the annual deficit is allowed for, further limited to not exceed 20% of the carbon mass in sapwood. If the C debt becomes larger, leaf and root biomass is reduced to satisfy tree allometry requirements. In this study, an alternative code explicitly accounting for storage of NSC was implemented as part of the annual allocation routine

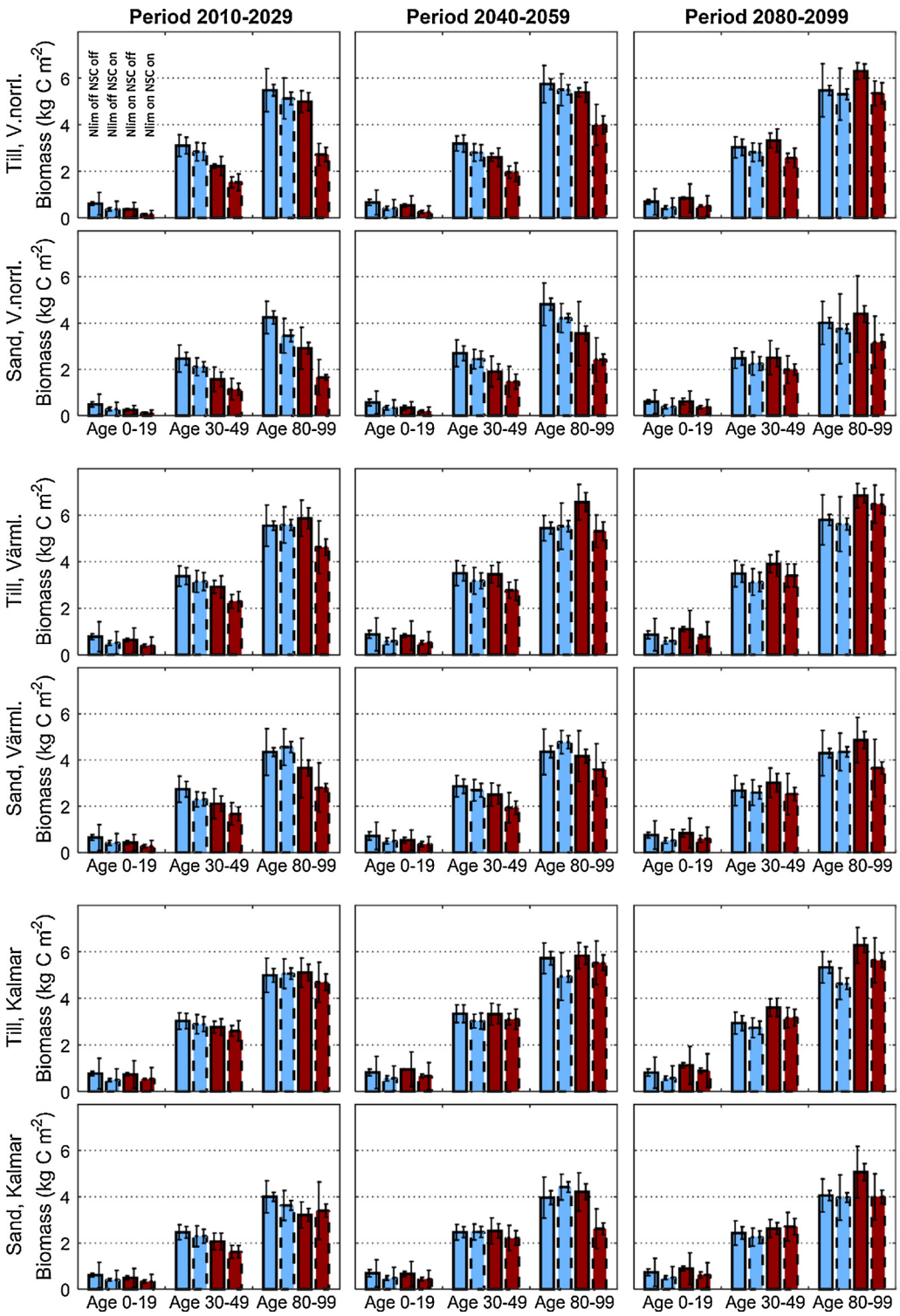


**Fig. 4.** Average carbon stored in biomass for 20 year periods and the 4 climate data sets for different periods, age-classes, soil types and counties. The four bars within each age-class represent the combinations of N cycling off (blue bars) or on (red bars), and NSC accounting off (solid contour line) or on (dashed line). The left error-bars show the variation of the mean ( ± one standard deviation) among model runs with four different climate model datasets, and the right error-bars show the inter-annual variation ( ± one standard deviation, mean of four model runs). (For interpretation of the references to colour in this figure legend, blue appears as grey and red as black in black and white print.)

simulated by the end of each year (NSC on, Eq. (1)). While the NSC storage has commonly been defined from measurements, i.e. in terms of concentration, it is the outcome in terms of altered pool sizes that is of key interest (Hartmann and Trumbore, 2016). This study therefor focuses on carbon pools rather than concentrations. The maximum NSC storage pool ($NSC_{max}$) was set to be twice as large as the pool of structural carbohydrates in the canopy, an approximation based on data on total leaf mass per NSC pool in above-ground xylem in evergreen coniferous tree species (Hoch et al., 2003). That is, the maximum storage is dynamically scaled in relation to the climate and nitrogen dependent tree allometry and annual growth. The allocation to NSC storage at time t ($NSC_t$) was calculated on the basis of the storage at previous time step (t-1), as the lowest positive amount of either the gap in NSC storage ($NSC_{max} - NSC_{t-1}$) or the amount of carbohydrates available for storage ($photosynthesis_t$ – $autotropic\_respiration_t$). The remaining carbohydrates were allocated to growth, $NPP_t$ (Eq. (2)).

$$NSC_t = NSC_{t-1} + \max(\min(NSC_{max} - NSC_{t-1}, photosynthesis_t - autotropic\_respiration_t), 0.0) \quad (1)$$

$$NPP_t = photosynthesis_t - autotropic\_respiration_t - (NSC_t - NSC_{t-1}) \quad (2)$$

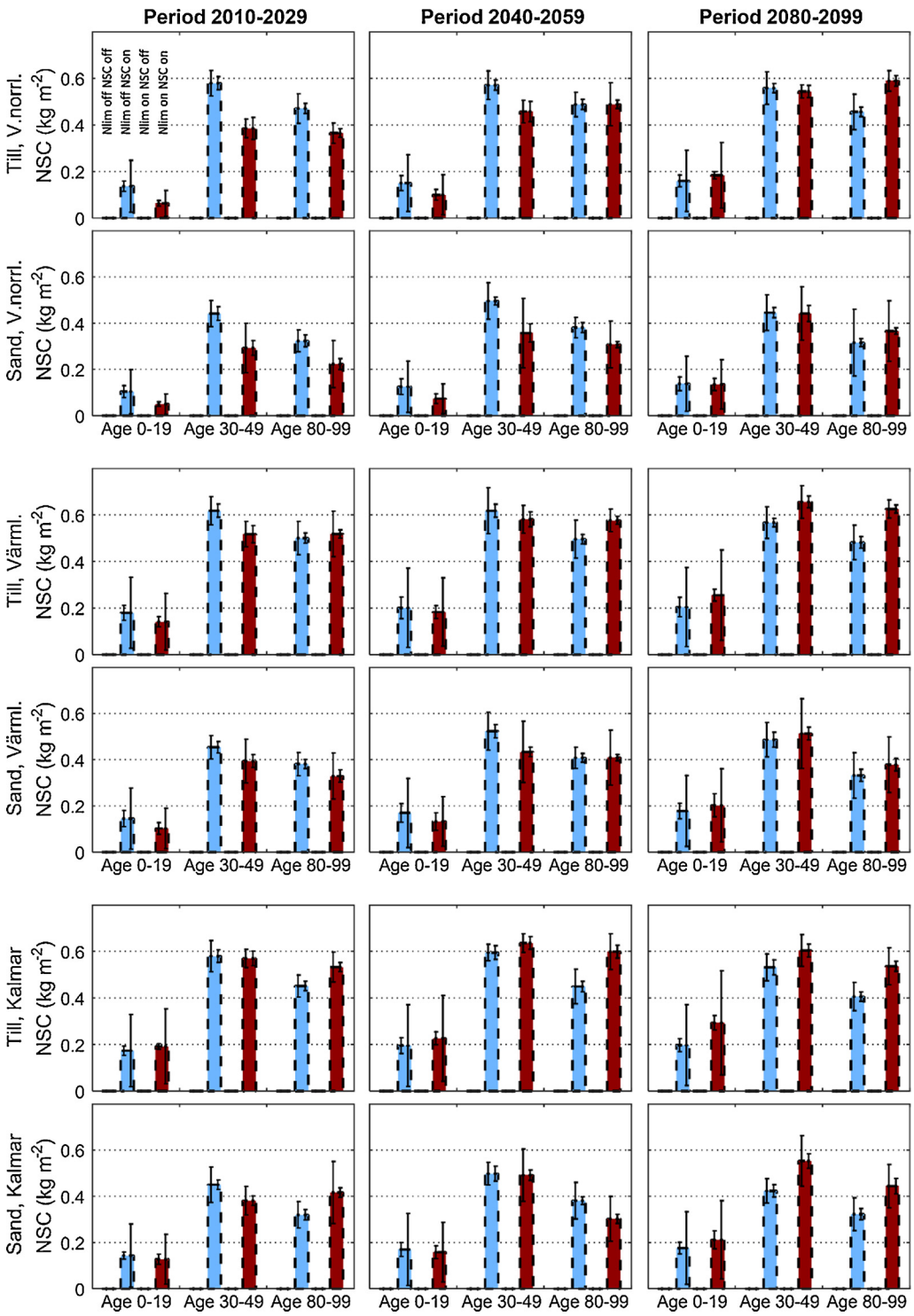


**Fig. 5.** Average non-structural C stores over 20 year periods and the 4 climate data sets for different periods, age-classes, soil types and counties. The four bars within each age-class represent the combinations of N cycling off (blue bars) or on (red bars), and NSC accounting off (solid contour line) or on (dashed line). The left error-bars show the variation of the mean ( ± one standard deviation) among model runs with four different climate model datasets, and the right error-bars show the inter-annual variation ( ± one standard deviation, mean of four model runs). (For interpretation of the references to colour in this figure legend, blue appears as grey and red as black in black and white print.)

### 2.4. Analysis of model simulations

Model output, in terms of monthly and annual NPP, biomass and soil water content (SWC), corresponding to model runs generated to cover all combinations of the seven factors, were included in the analysis of results. The result section includes information on these aspects in relation to site and soil specific conditions (***factor 1 and 2***), temporal aspects (***factor 3 and 4***), model parameterisation (***factor 5 and 6***) and selection of climate data (***factor 7***). Statistical analysis comparing the variation among factors were carried out in Matlab 2015a, using the ANOVAN function.

The analysis of NPP includes a comparison over years, to assess the net increase or decrease in primary production in response to altered climate conditions. An analysis of the winter NPP ($NPP_w$), calculated as a sum of the monthly NPP during October to February, generated a proxy of the wintertime autotrophic respiration. To account for the dependence of autotrophic respiration on total living biomass, which in turn can be influenced by the climate conditions, a normalised measure of the mean winter NPP ($NPP_{wn}$) was calculated as $NPP_w$ divided by the total biomass. The biomass was quantified as the carbon storage in living trees ($kg\,C\,m^{-2}$), including the amount of non-structural

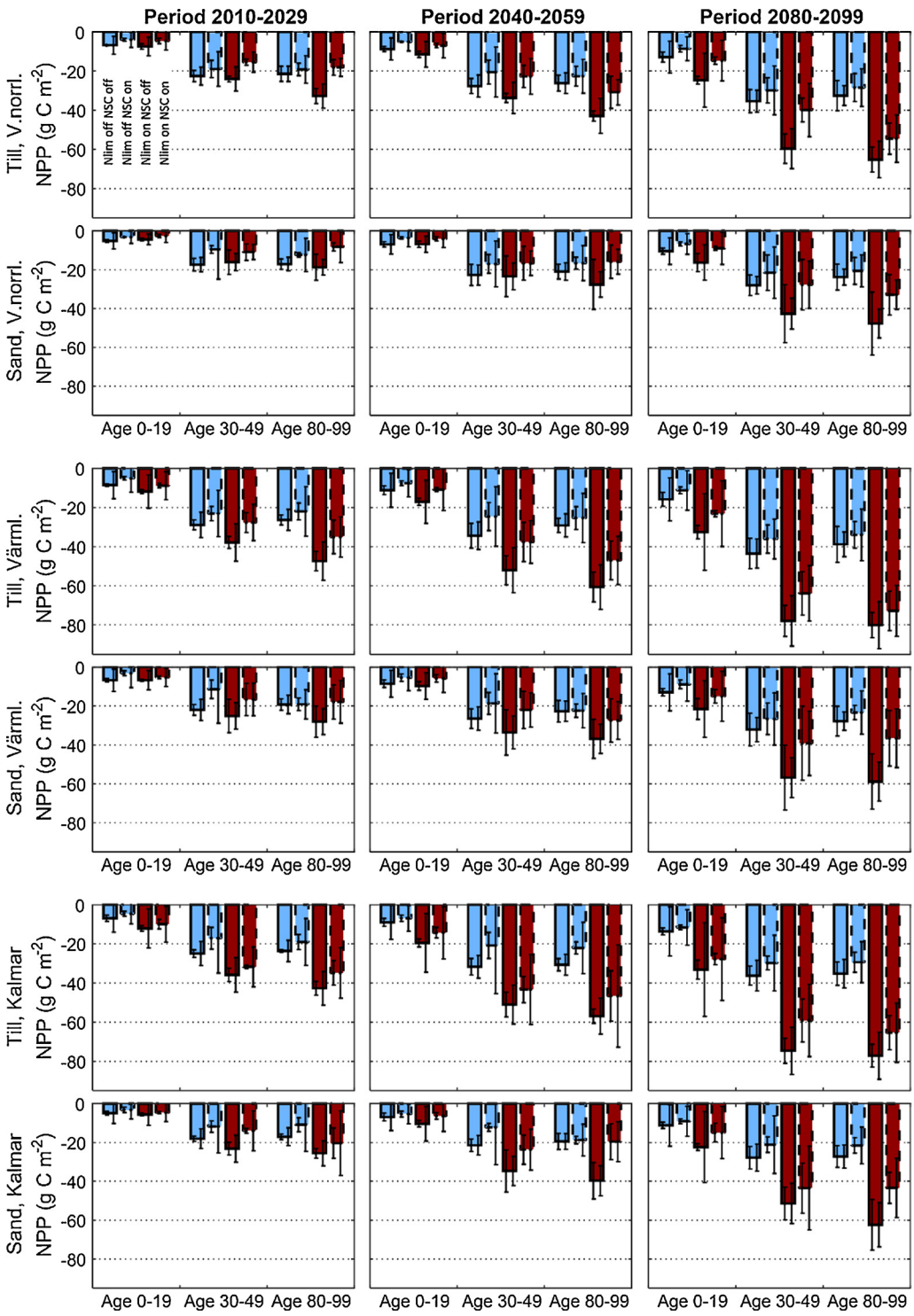


**Fig. 6.** Mean values of the total NPP for the darkest months (Oct–Feb) for 20 year periods over the 4 climate data sets for different periods, age-classes, soil types and counties. The four bars within each age-class represent the combinations of N cycling off (blue bars) or on (red bars), and NSC accounting off (solid contour line) or on (dashed line). The left error-bars show the variation of the mean ( ± one standard deviation) among model runs with four different climate model datasets, and the right error-bars show the inter-annual variation ( ± one standard deviation, mean of four model runs). (For interpretation of the references to colour in this figure legend, blue appears as grey and red as black in black and white print.)

carbohydrates (NSC, kg C $m^{-2}$). The relative soil water content (SWC) was calculated as the fraction of the water holding capacity in the upper soil layer that was filled with water. To generate a proxy of tree drought stress the frequency of months with SWC less than 0.2 over the 20-year periods was used (Lagergren and Lindroth, 2002). The result section includes drought frequency estimates for June, July and August as these are the months with highest likelihood of tree drought stress, and the complete dataset on SWC for the summer and winter months are presented in Supplement 1. The ensemble of model simulations were sequentially averaged over all but one factor (site, period, soil type, age class, N cycling, NSC accounting and climate data) to generate estimated averages of NPP, NSC and SWC.

## 3. Results

### 3.1. Simulated trends in production and biomass

The ensemble of LPJ-GUESS simulations, including the full range of parameter settings, indicated that the NPP ranges from 0.26 kg C $m^{-2}$ at the northernmost site in Västernorrland to 0.30–0.31 at the sites in Värmland and Kalmar, under current climate conditions. The simulation period averages were slightly higher (+0.03 kg C $m^{-2}$) (Table 3).

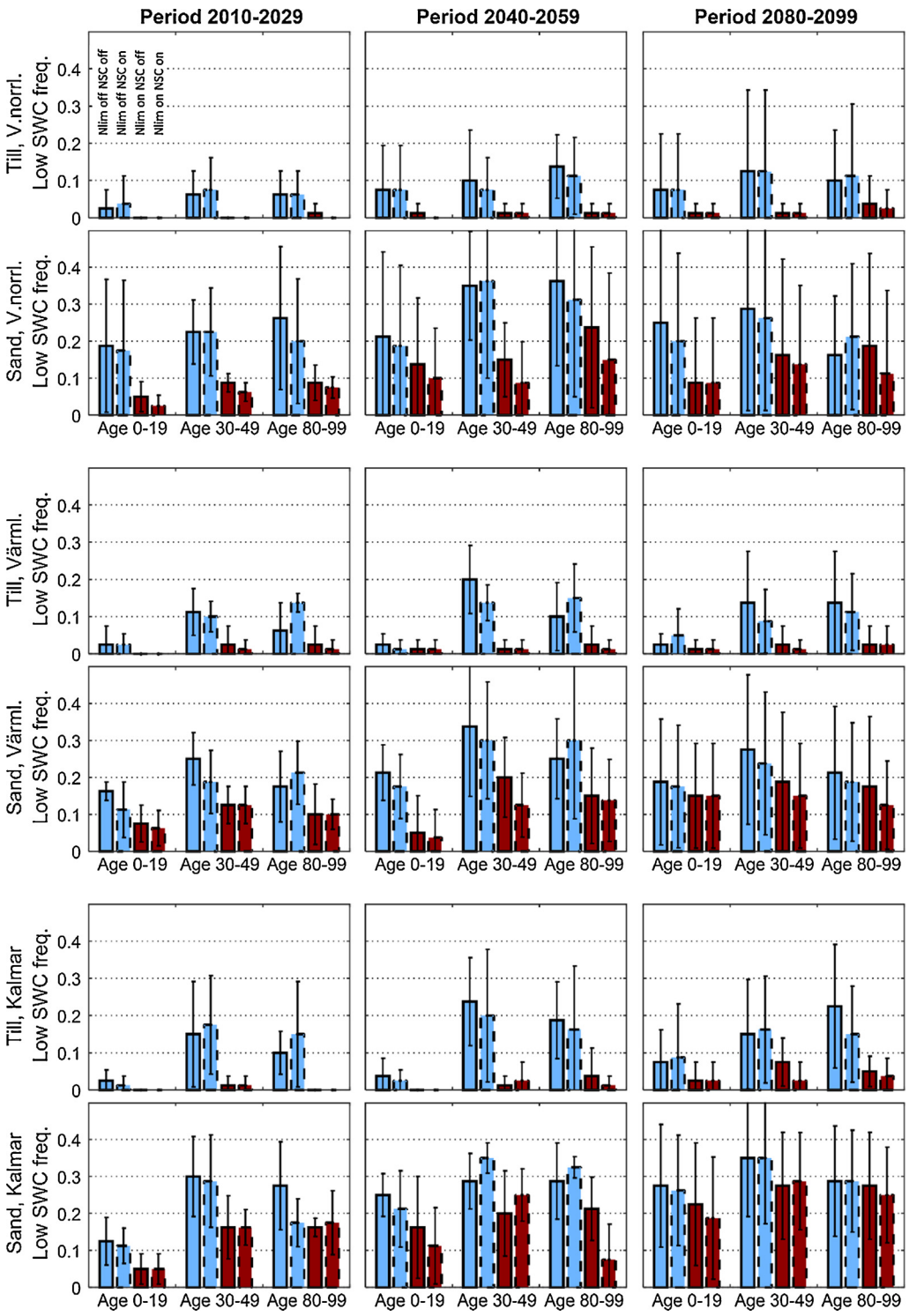


**Fig. 7.** Fraction of years with relative soil water content (SWC) in the upper layer < 0.2 in June for different 20-year periods, age-classes, soil types and counties. The four bars within each age-class represent the combinations of N cycling off (blue bars) or on (red bars), and NSC accounting off (solid contour line) or on (dashed line). The left error-bars show the variation of the mean ( ± one standard deviation) among model runs with four different climate model datasets, and the right error-bars show the inter-annual variation ( ± one standard deviation, mean of four model runs). (For interpretation of the references to colour in this figure legend, blue appears as grey and red as black in black and white print.)

The simulated productivity differed significantly between the two soil classes, being about 20% higher for conifer stands on till (0.33–0.36 kg C $m^{-2}$) than on sandy soils (0.18–0.25 kg C $m^{-2}$). In comparison with NPP estimates based on data from the Swedish national forest inventory (NFI, Nilsson and Corey, 2013), the modelled NPP was within the observed range for spruce and pine in Västernorrland and on sandy soils in Värmland but significantly lower for till soils in Värmland and all soils in Kalmar (Fig. 2).

The ensemble simulations indicated that NPP could increase on average by 10–15% at the three sites, comparing the end of the 21st century under RCP 8.5 with current climate conditions. The trend varied among sites and model settings (Fig. 3). The most pronounced increase over time, a doubling of NPP, was found for young trees (0–19 years old) in Västernorrland, when comparing the simulations with N cycling. In general, model simulations without N cycling indicated a less pronounced increase, with no additional increase or even a slight decrease (e.g. for the till soil in Kalmar) when comparing the near future with the far future (Fig. 3). Furthermore, the level of NPP was influenced by the forest stand-age. At all three sites the productivity was low for young trees, increasing over time until reaching a peak around the mid-ages, then entering a stage of slow decline as the trees grow older. The inter-annual variation in NPP was in the order of

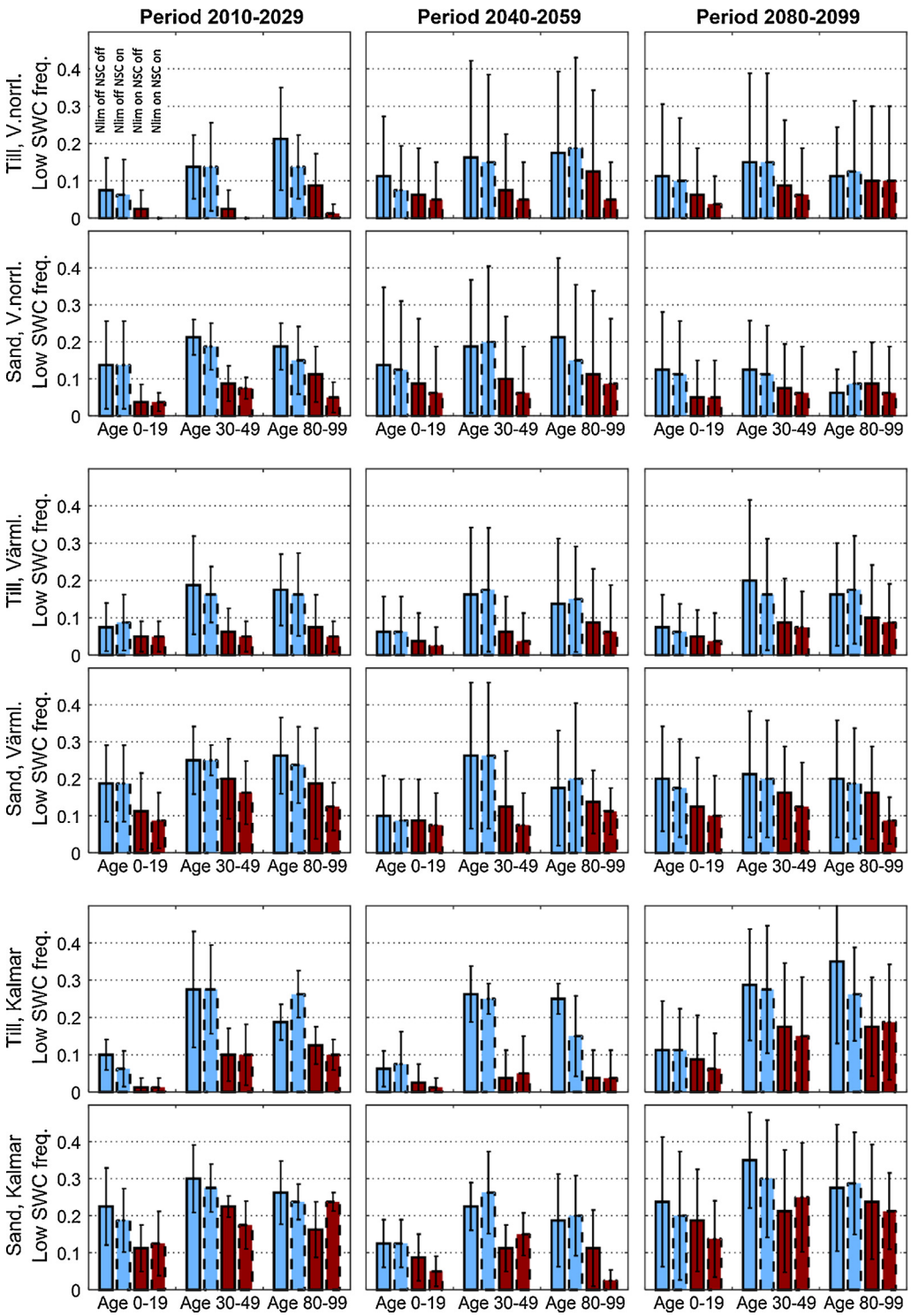


**Fig. 8.** Fraction of years with relative soil water content (SWC) in the upper layer < 0.2 in July for different periods, age-classes, soil types and counties. The four bars within each age-class represent the combinations of N cycling off (blue bars) or on (red bars), and NSC accounting off (solid contour line) or on (dashed line). The left error-bars show the variation of the mean ( ± one standard deviation) among model runs with four different climate model datasets, and the right error-bars show the inter-annual variation ( ± one standard deviation, mean of four model runs). (For interpretation of the references to colour in this figure legend, blue appears as grey and red as black in black and white print.)

10%, except for the 0–19 age-class for which the recovery from zero NPP at harvest generated a strong trend (and thereby a large variation) over years.

Model simulations with N cycling generated 18% lower NPP in Västernorrland than at the two other sites, whereas the NPP did not differ among sites in simulations without N cycling. The model simulations with "NSC on" generated slightly lower NPP than the model simulations not accounting for NSC (Table 3), and for the youngest age-class the NPP became substantially lower with NSC as a relatively large proportion of the photosynthate were allocated to NSC instead of growth (Fig. 3). The selection of climate model data influenced the simulated NPP, and simulations driven by the EC-earth climate data stood out as they generated 20–25% lower NPP than model runs with the other climate data sets, showing a covariance with low soil water content during summer (Table 3). The differences among model runs and trends over time observed for the NPP was in turn converted to differences in standing biomass (Fig. 4).

### 3.2. Non-structural carbohydrates

The levels of NSC (Fig. 5) were strongly related to LAI, as the maximum NSC storage was scaled in relation to the structural

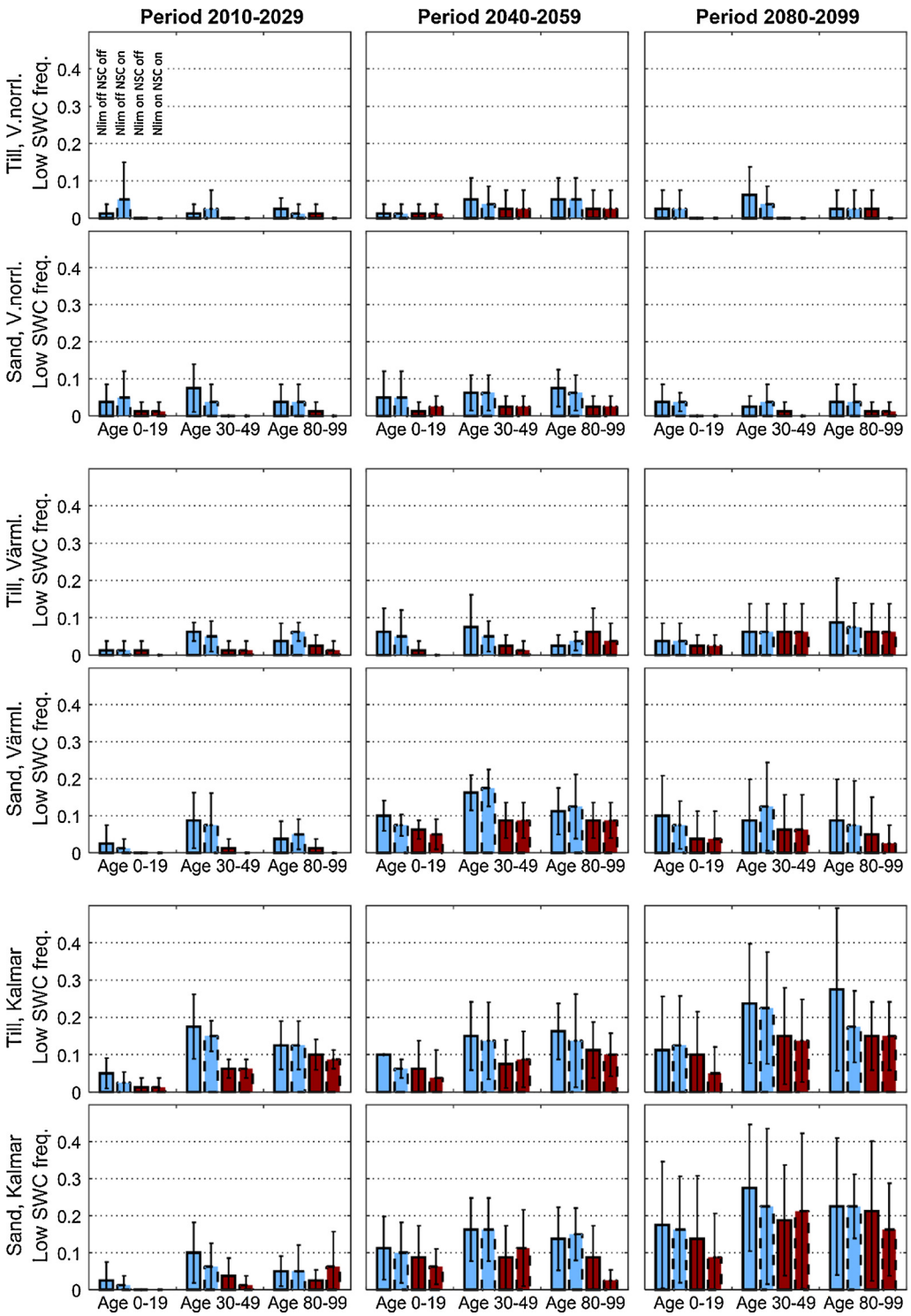


**Fig. 9.** Fraction of years with relative soil water content (SWC) in the upper layer < 0.2 in August for different periods, age-classes, soil types and counties. The four bars within each age-class represent the combinations of N cycling off (blue bars) or on (red bars), and NSC accounting off (solid contour line) or on (dashed line). The left error-bars show the variation of the mean ( ± one standard deviation) among model runs with four different climate model datasets, and the right error-bars show the inter-annual variation ( ± one standard deviation, mean of four model runs). (For interpretation of the references to colour in this figure legend, blue appears as grey and red as black in black and white print.)

carbohydrates of the canopy. The youngest trees therefore displayed the largest inter-annual variations in NSC, induced by the rapid growth and development over time. The allocation of NSC to storage, "NSC on", led to less leaf biomass and lower NPP estimates than "NSC off" (Table 3). The effect was generally most pronounced in combination with N cycling, resulting in the lowest estimates of NPP and biomass accumulation (Figs. 3 and 5). As inter-annual variations in climate conditions influenced the modelled NSC, the variation among model runs with different climate data sets was substantially larger than the between-year variation within a model run, especially for the sand soil (Fig. 5). The lowest NSC level of all simulations was 83% of maximum storage for middle aged forest and 88% for old forest, thus none of the model simulations indicated a major effect of combined stressful conditions that would lead to a substantially lowered carbohydrate storage over a period of years.

### 3.3. Tree winter respiration

The LPJ-GUESS simulations indicated that $NPP_w$ ranges from $-20.5$ g C m$^{-2}$ at the northernmost site in Västernorrland to $-25.9$ to $-27.5$ g C m$^{-2}$ at Kalmar and Värmland. Warmer winters can have a significant impact on the autotrophic respiration, and the model

**Table 4**
Fraction of years with mean monthly relative soil water content (SWC) in the upper layer < 0.2, a proxy of drought stress, for the three study sites and three summer months. The data from a multitude of LPJ-GUESS model runs have been averaged over all but one factor sequentially (soil type, period, age class, N limitation setting, NSC accounting and climate data).

| | Kalmar | | | Värmland | | | Västernorrland | | |
|---|---|---|---|---|---|---|---|---|---|
| Variable | Jun | Jul | Aug | Jun | Jul | Aug | Jun | Jul | Aug |
| 2010–2029 | 11% | 17% | 6% | 9% | 14% | 3% | 8% | 10% | 2% |
| 2040–2059 | 15% | 12% | 10% | 12% | 12% | 7% | 14% | 12% | 3% |
| 2080–2099 | 18% | 21% | 17% | 12% | 13% | 6% | 12% | 9% | 2% |

simulations, corresponding to RCP 8.5, showed that the C losses during the darkest months of winter (October to February) could become twice as high by end of the century as currently (Fig. 6, Table 3). The normalized winter respiration loss showed that the trees lose about 1% of their total biomass in the current climate, which can increase to 1.6% by 2080–2099 (Table 3). The NPP loss was higher for the till than the sand soil, both in absolute and relative terms. This is mainly attributable to differences in respiration level, influenced by N status and fraction of living biomass, as the autotrophic winter respiration was significantly higher for conifer stands on till than on sandy soils, also reflected by the normalised winter respiration values ($NPP_{wn}$) (Table 3). The modelled soil temperature is a factor that influences root respiration, however, this effect was considered negligible as the average difference in modelled soil temperature was 0.01 °C (root mean squared difference of 0.09 °C).

In relation to the tree size, the absolute and relative loss displayed opposite trends, with the amount of losses being higher in older forest and the relative loss being higher in young forest. That is, the relative loss decreases from approximately 0.4% in newly planted forest to around 0.15% in mature forest, with the loss in young forest being higher at higher latitudes as it takes longer time for the trees to reach a size at which the respiration levels off as a result of a decreasing sapwood to heartwood ratio.

Model runs with N cycling generated higher N content of sapwood and roots than model runs without N cycling, with the consequence that the model simulations displayed a higher sensitivity to elevated temperatures during the darkest months, as higher N content is linked to higher respiratory losses. There was no difference in the current climate for the northernmost site while the difference was more than 100% for the southern site by the end of the century (Fig. 6). Implementing NSC accounting resulted in less negative NPP during winter, and the model runs driven by different climate data sets ranged between $-13.1$ to $-11.6\ g\ kg^{-1}$ (Table 3).

### 3.4. Frequency of low soil water content

The simulated level of soil water content was highly dependent on the climate model data, with the regional climate model data sets originating from a dynamic downscaling of data from CanESM2 and EC-EARTH tending to generate lower SWC than data from CERFACS and IPSL for the last time period (Supplement 1, Figs. S1–S3). In this study a threshold of 0.2 was used as a proxy of drought stress, to enable a comparison among model runs in terms of projected impacts. The most pronounced difference among model runs was found for the month of July in Västernorrland, with the model run driven by EC-EARTH climate data indicating a substantially higher frequency of low SWC than the other climate data sets (28% compared with 2–5%). Furthermore, the model simulations indicated that the fraction of years with a mean monthly SWC in the upper layer being less than 0.2 ranged from 2 to 11% of the years in Västernorrland, 5–13% in Värmland, and 11–17% in Kalmar, generally being high in June and July, and substantially lower in August (Table 3). The frequency of low SWC was about three times higher for sand than till in June, whereas the differences were less pronounced in July (about 1.4 times higher) and August (about 1.2 times higher) (Fig. 7–9, Table 3). The simulations also indicated that younger trees were significantly less likely to experience drought conditions than older trees (Table 3).

In Kalmar the drought frequency consistently increased over time in the RCP 8.5 scenario, but for Värmland there was no further increase after the 2040–2059 period, and Västernorrland indicated a slight decline for the last period (Table 4). Especially for the till soil, simulations with N cycling implied fewer years with low SWC, with the largest difference found for June in Kalmar, 2040–2059 (low SWC in one out of fifty years compared with one out of five years, Fig. 7). Model simulations with NSC indicated 1–2% lower frequency of low SWC, likely related to a slightly lower NPP.

## 4. Discussion

Climate change, including changes in the frequency and severity of extreme events, is likely to influence forest stand productivity and vitality in Sweden (Eriksson et al., 2015). In this study we combined regional ecosystem modelling with an analysis of local differences in soil conditions, using a dynamic approach to assess potential climate change impacts, which cannot be accounted for by traditional empirical forest management models. Differences in climate vulnerability among forest stands were assessed, using a sub-ensemble of bias-corrected climate model data, corresponding to RCP 8.5. The simulations showed that the productivity of boreal conifer forests in Sweden is influenced by the fine interplay between site-specific temperature conditions and precipitation. The model results depicted that local differences in soil conditions have a large impact on the productivity, mediated by soil water and nutrient contents, which is well known from the empirical relations commonly used for estimations of production potential (Hägglund and Lundmark, 1977). Furthermore, the model analysis indicated that model setting explicitly taking NSC and N dynamics into account influences the NPP estimates.

### 4.1. Model performance

The growth of the boreal forests in northern Europe is mainly constrained by the dark and cold winter season (Nemani et al., 2003). Furthermore, fertilisation and irrigation experiments of Norway spruce forest stands have indicated that water availability during growing season can be more of a limiting factor for tree growth in the south than in the north of Sweden (Bergh et al., 1999). This is in line with the findings of this study, with lowest productivity at the northernmost site (Västernorrland), and similar productivity levels at the south site and the central site (Kalmar and Värmland), as the benefit of a slightly longer growing season at the south site was offset by a higher frequency of drought stress.

The LPJ-GUESS version without N cycling has been found to generate NPP estimates that are similar to other terrestrial carbon cycle models and data from FACE experiments (Piao et al., 2013). However, the modelled NPP was generally at the lower end compared with observed forest productivity, being closer to the NFI based NPP estimates of the northern site than of the southern site and closer to Scots pine forest than Norway spruce forest (Fig. 2). This generated an age-class specific modelled biomass (Fig. 4) that was lower than indicated by forest monitoring (Table 2). This is in line with a recent study, in which NPP estimates similar to LPJ-GUESS were obtained using Biome-BGC, arguing that the inability to capture the latitudinal gradient in productivity of Swedish forests could be due to limited parameter calibration (Dubber et al., 2017). That is, despite mechanistic properties, the vegetation models are likely not capable of capturing the species specific adaptations to environmental conditions, such as latitudinal gradients in light and temperature (Olsson and Jönsson, 2014).

Carbon-nitrogen interactions can have a significant influence on the

simulated response to climate change and increased ambient $CO_2$ concentration (Piao et al., 2013), and for all three sites there was an interaction between the N cycling setting and climate period. Model runs with N cycling enabled generated slightly lower NPP for 2010–2029 and slightly higher NPP for 2080–2099, compared with model runs without N cycling. The effect was most pronounced for the youngest age class (c.f. Fig. 3), which is related to that the trees became more light limited without N cycling due to a lower value of $\alpha_a$ and a decreasing trend over the years in incoming shortwave radiation (Lagergren and Jönsson, 2017). N cycling influenced the model estimates also in terms of low soil water content and risk of drought stress. Model simulations without N cycling indicated a significantly higher frequency of events with low soil water content than simulations with N cycling, due to a lower water use efficiency linked to the lower value of $\alpha_a$ (Smith et al., 2014).

The NSC accounting implemented in this study generated slightly lower NPP values, caused by a carry-over effect between years. This is a result of more restricted growth in years when water was a limiting factor for tree photosynthesis, resulting in less carbon allocated to crown development, which reflects current understanding of NSC allocation principles (Hartmann and Trumbore, 2016). Furthermore, the simulated risk of summer drought, as indicated by a low SWC, differed significantly among model runs with different climate data sets (Supplement 1, Figs. S1–S3), showing the importance of using an ensemble of climate model data to identify key uncertainties associated with future projections (Littell et al., 2011).

### 4.2. Trends related to climate change

Forest growth potential in Sweden has been predicted to increase in response to a temperature induced lengthening of the growing season (Bergh et al., 2003; Eriksson et al., 2015; Koca et al., 2006). This study confirmed this, however it also indicated that the productivity increase will be partly offset by higher autotrophic respiration in winter and higher frequency of drought stress in summer. That is, the NSC storage of coniferous tree species can be reduced during late winter and early spring if the temperature dependent respiration rate is high while the light dependent photosynthesis is low or inactive (Kalberer et al., 2006). The response to drought stress will depend on the length and intensity of the event, as growth limitation caused by mild drought results in accumulation of carbohydrates while the amount of non-structural carbohydrates can become reduced during a more severe drought stress (McDowell, 2011).

Low levels of NSC can trigger tree mortality, separately or in combination with drought stress (Galiano et al., 2011; Hartmann and Trumbore, 2016; McDowell, 2011). However, no indication of cumulative environmental stress leading to severely depleted NSC storage over years was found in this study, which included four sets of climate model data generating 80 simulations years for each time period of 20 years. The estimated size of $NSC_{max}$, based on a few central Europe trees sampled in 1999–2002 (Hoch et al., 2003), is subjected to uncertainties as the NSC pool can show strong seasonal and interannual variations (Hartmann and Trumbore, 2016). However, the lowest NSC level found in this study, 83% of the annual maximum NSC pool, is clearly above the suggested minimum level of ~46% for coniferous trees (Adams et al., 2017; Martinez-Vilalta et al., 2016), indicating that the results of this modelling study are robust in relation to the $NSC_{max}$ parameterization. That is, the trees are not likely to primarily suffer from carbon depletion but may during shorter periods of reduced NSC availability become more susceptible to attacks by secondary agents, such as bark beetles (Rouault et al., 2006).

The result of this study is indicative of the study region only, as northern Europe is less vulnerable to sever drought stress than southern Europe. Climate model projections indicate that this pattern will remain also in a warmer climate as there is medium confidence that climate change will lead to annual precipitation increases in northern Europe, it is likely that winter mean temperature will rise more in northern than southern Europe, and summer warming is likely to become more intense in southern than northern Europe (IPCC, 2013). At the local scale soil conditions can modify forest exposure to climate extremes and risk of forest damage. The ecosystem model simulation showed that Norway spruce on sandy soils were more exposed to drought stress, while Norway spruce planted on till soils were more exposed to high water saturation during winter (Supplement 1, Figs. S4–S6) which in combination with a lower probability of frozen soil conditions in a warmer climate will make them vulnerable to uprooting during a storm event (Lagergren et al., 2012; Seidl et al., 2011). Planting Norway spruce trees on sandy soil, better suited for Scots pine, may thus add to the landscape vulnerable to bark beetle attacks by increasing the amount of forest susceptible to drought stress. The model simulations indicated that middle age forests are somewhat more sensitive to stressful weather conditions than younger or older forests, due to a generally higher leaf biomass and thereby higher water requirement. Problems associated with unsuitable tree-site matching, i.e. planting Norway spruce trees on sandy soil more frequently exposed to summer drought, may not become apparent until the forest stand is middle-aged (Rouault et al., 2006). Climate change may worsen the outcome via an altered frequency and intensity of heatwaves and drought spells (SOU, 2007), which can influence the risk of successful spruce bark beetle attacks both via altered tree defence capacity (Christiansen et al., 1987) and altered insect phenology, caused by a temperature dependent shift from predominantly one to two generations per year in Sweden (Jönsson et al., 2011; Jönsson et al., 2012).

## 5. Conclusions

Model-derived knowledge on forest vulnerability to abiotic stress factors is needed to assess potential future risks and identify suitable adaptation strategies at the landscape level. In this study we applied an ecosystem model to address questions related to climate change and forest stand development on two soil texture classes, being managed as Norway spruce monocultures. Model runs with four different climate data sets and three sites indicated that the productivity increase, induced by a warmer climate leading to a longer growing season in Sweden, will be partly offset by a higher frequency of drought stress in summer and warm winters with elevated autotrophic respiration. The results indicated that non-structural carbohydrate depletion caused by cumulative environmental stress is less likely to become a primary cause of tree mortality in Sweden, but periods with low NSC levels may link to temporary reductions in tree defence capacity.

## Acknowledgements

This study was financially supported by FORMAS through the project Climate change impact on tree defence capacity (2010-822). We are grateful to R. Wilcke for assistance with selecting climate model data.

## Appendix A. Supplementary data

Supplementary material related to this article can be found, in the online version, at doi:https://doi.org/10.1016/j.ecolmodel.2018.06.023.

## References

Adams, H.D., et al., 2017. A multi-species synthesis of physiological mechanisms in drought-induced tree mortality. Nat. Ecol. Evol. 1 (9), 1285–1291.
Archaux, F., Wolters, V., 2006. Impact of summer drought on forest biodiversity: what do we know? Ann. For. Sci. 63 (6), 645–652.
Bergh, J., Linder, S., Lundmark, T., Elfving, B., 1999. The effect of water and nutrient availability on the productivity of Norway spruce in northern and southern Sweden. For. Ecol. Manage. 119 (1–3), 51–62.
Bergh, J., et al., 2003. Modelling the short-term effects of climate change on the

productivity of selected tree species in Nordic countries. For. Ecol. Manage. 183 (1-3), 327–340.
Bergquist, J., Ekö, P.-M., Elving, B., Johansson, U., Thuresson, T., 2005. Jämförelse av produktionspotential mellan tall, gran och björk på samma ståndort. Swedish Forest Agency Rapport 2005, vol. 19 32 pp.
Bergqvist, J., 2016. Risk med gran på tallmark. Skogseko 2016 (4), 28.
Bergqvist, G., Bergström, R., Edenius, L., 2001. Patterns of stem damage by moose (Alces alces) in young Pinus sylvestris stands in Sweden. Scand. J. For. Res. 16 (4), 363–370.
Bergström, R., Bergqvist, G., 1999. Large herbivore browsing on conifer seedlings related to seedling morphology. Scand. J. For. Res. 14 (4), 361–367.
Breda, N., Huc, R., Granier, A., Dreyer, E., 2006. Temperate forest trees and stands under severe drought: a review of ecophysiological responses, adaptation processes and long-term consequences. Ann. For. Sci. 63 (6), 625–644.
Chapin, F.S., Schulze, E.D., Mooney, H.A., 1990. The ecology and economics of storage in plants. Annu. Rev. Ecol. Syst. 21, 423–447.
Christiansen, L., 2014. Swedish Statistical Yearbook of Forestry 2014. Swedish Forest Agency, Jönköping978-91-87535-05-5 368 pp.
Christiansen, E., Bakke, A., 1997. Does drought really enhance Ips typo graphus epidemics?-A scandinavian perspective. In: Grégoire, J.C., Liebhold, A.M., Stephen, F.M., Day, K.R., Salom, S.M. (Eds.), Proceedings: Integrating Cultural Tactics into the Management of Bark Beetle and Reforestation Pests. US DA Forest Service General Technical Report NE-236, pp. 163–171.
Christiansen, E., Waring, R.H., Berryman, A.A., 1987. Resistance of conifers to bark beetle attack: searching for general relationships. For. Ecol. Manage. 22 (1–2), 89–106.
The spruce bark beetle of Eurasia. In: Christiansen, E., Bakke, A. (Eds.), Dynamics of Forest Insect Populations; Patterns, Causes, Implications. Plenum Publishing Corporation, New York 479–503 pp.
Desprez-Loustau, M.L., Marcais, B., Nageleisen, L.M., Piou, D., Vannini, A., 2006. Interactive effects of drought and pathogens in forest trees. Ann. For. Sci. 63 (6), 597–612.
Dubber, W., Eklundh, L., Lagergren, F., 2017. Comparing field inventory with mechanistic modelling and light-use efficiency modelling based approaches for estimating forest net primary productivity at a regional level. Boreal Eniviron. Res. 22, 337–352.
Eriksson, H., et al., 2015. Effekter av ett förändrat klimat – SKA 15. Skogsstyrelsen Rapport 12-2015.
Franceschi, V.R., Krokene, P., Christiansen, E., Krekling, T., 2005. Anatomical and chemical defenses of conifer bark against bark beetles and other pests. New Phytol. 167 (2), 353–376.
Galiano, L., Martinez-Vilalta, J., Lloret, F., 2011. Carbon reserves and canopy defoliation determine the recovery of Scots pine 4 yr after a drought episode. New Phytol. 190 (3), 750–759.
Guerard, N., Maillard, P., Brechet, C., Lieutier, F., Dreyer, E., 2007. Do trees use reserve or newly assimilated carbon for their defense reactions? A C-13 labeling approach with young Scots pines inoculated with a bark-beetle-associated fungus (Ophiostoma brunneo ciliatum). Ann. For. Sci. 64 (6), 601–608.
Hägglund, B., Lundmark, J.-E., 1977. Site index estimation by means of site properties: Scots pine and Norway spruce in Sweden. Studia Forestalia Suecica 138, 1–38.
Hartmann, H., Trumbore, S., 2016. Understanding the roles of nonstructural carbohydrates in forest trees—from what we can measure to what we want to know. New Phytol. 211 (2), 386–403.
Haxeltine, A., Prentice, I.C., 1996. BIOME3: an equilibrium terrestrial biosphere model based on ecophysiological constraints, resource availability, and competition among plant functional types. Global Biogeochem. Cycles 10 (4), 693–709.
Hoch, G., Richter, A., Korner, C., 2003. Non-structural carbon compounds in temperate forest trees. Plant Cell Environ. 26 (7), 1067–1081.
IPCC, 2013. Climate change 2013: the physical science basis. Contribution of Working Group I to the Fifth Assessment Report of the Intergovernmental Panel on Climate Change. Cambridge University Press, Cambridge, United Kingdom and New York, NY, USA.
Jönsson, A.M., Harding, S., Krokene, P., Lange, H., Lindelöw, A., Økland, B., Ravn, H.P., Schroeder, L.M., 2011. Modelling the potential impact of global warming on Ips typographus voltinism and reproductive diapause. Clim. Change 109 (3-4), 695–718.
Jönsson, A.M., Schroeder, L.M., Lagergren, F., Anderbrant, O., Smith, B., 2012. Guess the impact of Ips typographus—an ecosystem modelling approach for simulating spruce bark beetle outbreaks. Agric. For. Meteorol. 166, 188–200.
Jönsson, A.M., Lagergren, F., Smith, B., 2015. Forest management facing climate change—an ecosystem model analysis of adaptation strategies. Mitig. Adapt. Strat. For. Global Change 20 (2), 201–220.
Kalberer, S.R., Wisniewski, M., Arora, R., 2006. Deacclimation and reacclimation of cold-hardy plants: current understanding and emerging concepts. Plant Sci. 171 (1), 3–16.
Koca, D., Smith, B., Sykes, M.T., 2006. Modelling regional climate change effects on potential natural ecosystems in Sweden. Clim. Change 78 (2–4), 381–406.
Kotlarski, S., et al., 2014. Regional climate modeling on European scales: a joint standard evaluation of the EURO-CORDEX RCM ensemble. Geosci. Model. Dev. 7 (4), 1297–1333.
Lagergren, F., Jönsson, A.M., 2017. Ecosystem model analysis of multi-use forestry in a changing climate. Ecosyst. Serv. 26, 209–224.
Lagergren, F., Lindroth, A., 2002. Transpiration response to soil moisture in pine and spruce trees in Sweden. Agric. For. Meteorol. 112 (2), 67–85.
Lagergren, F., Jönsson, A.M., Blennow, K., Smith, B., 2012. Implementing storm damage in a dynamic vegetation model for regional applications in Sweden. Ecol. Modell. 247, 71–82.
Lamarque, J.F., et al., 2010. Historical (1850-2000) gridded anthropogenic and biomass burning emissions of reactive gases and aerosols: methodology and application. Atmosph. Chem. Phys. 10 (15), 7017–7039.
Lamarque, J.F., et al., 2011. Global and regional evolution of short-lived radiatively-active gases and aerosols in the representative concentration pathways. Clim. Change 109 (1-2), 191–212.
Lehtonen, A., Makipaa, R., Heikkinen, J., Sievanen, R., Liski, J., 2004. Biomass expansion factors (BEFs) for Scots pine, Norway spruce and birch according to stand age for boreal forests. For. Ecol. Manage. 188 (1-3), 211–224.
Littell, J.S., McKenzie, D., Kerns, B.K., Cushman, S., Shaw, C.G., 2011. Managing uncertainty in climate-driven ecological models to inform adaptation to climate change. Ecosphere 2 (9), art102.
Marini, L., et al., 2017. Climate drivers of bark beetle outbreak dynamics in Norway spruce forests. Ecography. http://dx.doi.org/10.1111/ecog.02769.
Martinez-Vilalta, J., et al., 2016. Dynamics of non-structural carbohydrates in terrestrial plants: a global synthesis. Ecol. Monogr. 86 (4), 495–516.
McDowell, N.G., 2011. Mechanisms linking drought, hydraulics, carbon metabolism, and vegetation mortality. Plant Physiol. 155 (3), 1051–1059.
Moss, R.H., et al., 2010. The next generation of scenarios for climate change research and assessment. Nature 463 (7282), 747–756.
Nemani, R.R., et al., 2003. Climate-driven increases in global terrestrial net primary production from 1982 to 1999. Science 300 (5625), 1560–1563.
Netherer, S., Ehn, M., Blackwell, E., Kirisits, T., 2016. Defence reactions of mature Norway spruce (Picea abies) before and after inoculation of the blue-stain fungus Endoconidiophora polonica in a drought stress experiment. Lesn. Cas. - For. J. 62 (4), 169–177.
Nilsson, P., Corey, N., 2013. Forestry Statistics 2013 - Official Statistics of Sweden. Arkitektkopia, AB, Umeå 162 pp.
Olsson, C., Jönsson, A.M., 2014. Process-based models not always better than empirical models for simulating budburst of Norway spruce and birch in Europe. Glob. Change Biol. 20 (11), 3492–3507.
Piao, S., et al., 2013. Evaluation of terrestrial carbon cycle models for their response to climate variability and to CO2 trends. Glob. Change Biol. 19 (7), 2117–2132.
Rosengren, R., Stjernquist, I., 2004. Gå på djupet! Om rotdjup och rotproduktion i olika skogstyper. SUFOR, Lund91-576-6617-2 55 pp.
Rouault, G., et al., 2006. Effects of drought and heat on forest insect populations in relation to the 2003 drought in Western Europe. Ann. For. Sci. 63 (6), 613–624.
Sandström, F., Petersson, H., Kruys, N., Ståhl, G., 2007. Biomass conversion factors (density and carbon concentration) by decay classes for dead wood of Pinus sylvestris, Picea abies and Betula spp. in boreal forests of Sweden. For. Ecol. Manage. 243 (1), 19–27.
Seidl, R., Rammer, W., Jaeger, D., Lexer, M.J., 2008. Impact of bark beetle (Ips typographus L.) disturbance on timber production and carbon sequestration in different management strategies under climate change. For. Ecol. Manage. 256 (3), 209–220.
Seidl, R., et al., 2011. Modelling natural disturbances in forest ecosystems: a review. Ecol. Modell. 222 (4), 903–924.
Smith, B., Prentice, I.C., Sykes, M.T., 2001. Representation of vegetation dynamics in the modelling of terrestrial ecosystems: comparing two contrasting approaches within European climate space. Global Ecol. Biogeogr. 10 (6), 621–637.
Smith, B., et al., 2014. Implications of incorporating N cycling and N limitations on primary production in an individual-based dynamic vegetation model. Biogeosciences 11 (7), 2027–2054.
SOU, 2007. Sweden facing climate change—threats and opportunities. Swedish Government Official Report, 2007, vol. 60. pp. 679.
Wilcke, R.A.I., Bärring, L., 2016. Selecting regional climate scenarios for impact modelling studies. Environ. Modell. Softw. 78, 191–201.
Wilcke, R.A.I., Mendlik, T., Gobiet, A., 2013. Multi-variable error correction of regional climate models. Clim. Change 120 (4), 871–887.
Zhao, T., et al., 2011. Induced terpene accumulation in Norway spruce inhibits bark beetle colonization in a dose-dependent manner. PLoS One 6 (10), e26649.